

# BridgeEQA: Virtual Embodied Agents for Real Bridge Inspections

Subin Varghese, Joshua Gao, Asad Ur Rahman, Vedhus Hoskere

University of Houston

4226 MLK Blvd, Houston, TX 77204

{srvargh2, jkgao, aurahman}@cougarnet.uh.edu, vhoskere@uh.edu

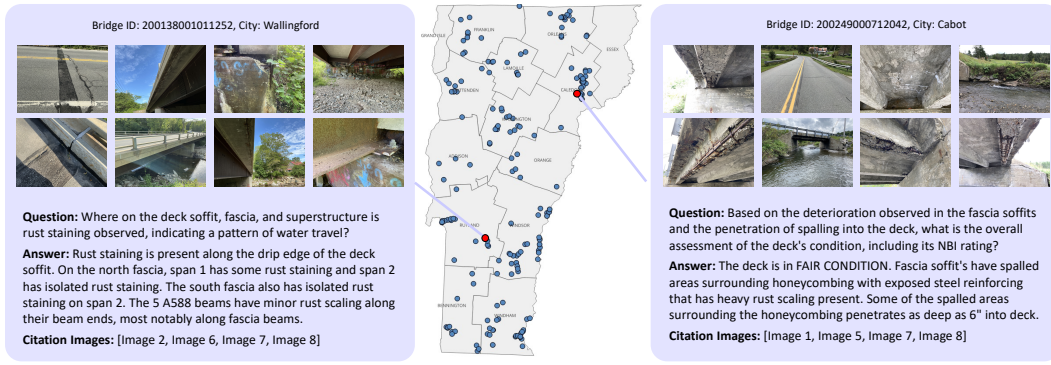


Figure 1. **BridgeEQA: Open-Vocabulary Embodied Question Answering for bridge inspection.** Two example scenes from our benchmark showing questions that require synthesizing visual evidence across multiple egocentric images to assess bridges.

## Abstract

Deploying embodied agents that can answer questions about their surroundings in realistic real-world settings remains difficult, partly due to the scarcity of benchmarks that faithfully capture practical operating conditions. We propose infrastructure inspection as a compelling domain for open-vocabulary Embodied Question Answering (EQA): it naturally demands multi-scale reasoning, long-range spatial understanding, and complex semantic relationships, while offering unique evaluation advantages via standardized National Bridge Inventory (NBI) condition ratings (0-9), professional inspection reports, and egocentric imagery.

We introduce BridgeEQA, a benchmark of 2,200 open-vocabulary question-answer pairs (in the style of OpenEQA) grounded in professional inspection reports across 200 real-world bridge scenes with 47.93 images on average per scene. Questions require synthesizing visual evidence across multiple images and aligning responses with NBI condition ratings. We further propose a new EQA metric Image Citation Relevance to evaluate the ability of a model to cite relevant images.

Evaluations of state-of-the-art vision-language models reveal substantial performance gaps under episodic memory EQA settings. To address this, we propose Embod-

ied Memory Visual Reasoning (EMVR), which formulates inspection as sequential navigation over an image-based scene graph: images are nodes, and an agent takes actions to traverse views, compare evidence, and reason within a Markov decision process. EMVR shows strong performance over the baselines. We publicly release both the dataset and code.

## 1. Introduction

When stacking a tower of blocks as a child, we learn not only to build upward but to probe structure: which elements are load-bearing, which are redundant, and how removing one piece will redistribute forces. After even a brief examination, we form a mental model of the tower's geometry and dependencies. Professional bridge inspectors exercise this same spatial reasoning at scale. As they move through egocentric viewpoints, they synthesize visual evidence via a systematic process guided by standards like the American Association of State Highway and Transportation Officials (AASHTO) Manual for Bridge Element Inspection (MBEI). This requires decomposing the structure into a hierarchy of components and elements, assessing condition objectively, and documenting these findings with structured outputs per the Specifications for the National Bridge In-

ventory (SNBI).

Recent embodied and spatial question answering benchmarks for vision-language models (VLMs) [12, 30, 46] tend to evaluate reasoning over small spatial extents and relatively simple queries, such as object counts or relative positions in constrained scenes. While these benchmarks are invaluable for measuring core capabilities, they under-represent challenges found in real-world deployments. These challenges include vast spatial extents, hierarchical organization from global overviews to fine-grained details, heterogeneous imaging conditions, and reconciling observations with domain-specific criteria.

We propose infrastructure inspection, and bridge inspection in particular, as a compelling testbed for Embodied Question Answering (EQA). First, the domain naturally demands multi-scale reasoning, long-range spatial understanding, and complex semantic relationships between structural components that many times require multiple images to resolve. Second, a large volume of real-world data with expert annotations already exists in the form of professional inspection reports which include egocentric imagery and inspector notes regarding the structure. Third, standardized numerical ratings of components based on the National Bridge Inventory (NBI) scale [15] provide objective numerical values that can be used to evaluate agents’ responses to directly compare to expert human inspectors. Finally, advancements in this domain have high potential for real-world impact as aging infrastructure requires regular, large-scale assessments that are labor-intensive and costly [5, 15].

To this end, we introduce **BridgeEQA**, a benchmark of 2,200 open-vocabulary question-answer pairs, in the style of Episodic Memory EQA (EM-EQA) from [30] OpenEQA, with real imagery from bridge inspection reports across 200 bridge scenes, with an average of 47.93 images per scene. Questions require aggregating visual evidence across multiple views and aligning responses with NBI condition ratings. Motivated by bridge inspection practice, where inspectors must justify numerical ratings with specific photographic evidence [15, 39], we evaluate condition rating accuracy and propose a new metric **Image Citation Relevance** that semantically evaluates the set of images a model cites to support its answer against a reference set of images. Finally, following existing open-vocabulary QA evaluation protocols [28, 30, 50], we also evaluate the open-vocabulary text response via LLM-as-a-judge [50]. Together, these metrics holistically evaluate the model in terms of the alignment of open-vocabulary answers to ground truth answers, the relevance and faithfulness of the cited visual evidence, and agreement with expert human inspectors.

Evaluations using three state-of-the-art proprietary vision-language models, Gemini 2.5 Flash, Gemini 2.5 Flash-Lite, and Grok 4 Fast, with the strongest base-

line method from OpenEQA for EM-EQA, Multi-Frame VLM [30], revealed sizable performance gaps. Considering prior works have documented a positional bias in long-context LLMs toward the beginning or end of a sequence [6, 9, 19, 21, 23, 27], we theorized this may be the cause for poor performance. Therefore, we devised a reformulation of the Multi-Frame VLM approach for EM-EQA to be akin to an active Embodied agent in an Active EQA (A-EQA) setting. To do so, we direct the Embodied agent to dynamically retrieve context using a scene graph representation, in which images are nodes rather than objects, serving as an allocentric map. The Embodied agent must then make function calls to take actions such as to move to different nodes, analyze multiple images, analyze an image, and return a response in a Markov decision process (MDP). This dynamically allows the agent to select and promote mid-sequence information to the front of the context window, mitigating positional bias, Figure 2. We call this method Embodied Memory Visual Reasoning (EMVR) as it is akin to an agent reasoning over its memory. We find EMVR improves condition rating accuracy  $\pm 1$  by 9.34 percentage point, Image Citation Relevance by 20.2 percentage point, and Answer Correctness by 7.2 percentage point over Multi-Frame VLM using Grok 4 Fast. In summary, this work makes the following contributions:

1. **BridgeEQA benchmark with expert-grounded supervision.** We release **BridgeEQA**, a real-world EQA dataset for infrastructure inspection comprising 2,200 questions over 9,586 images from 200 bridge scenes across 73 towns, averaging 47.93 images per scene.
2. **Metrics for inspection EQA agent evaluation** We introduce a new EQA metric *Image Citation Relevance* to assess semantic similarity between cited images of an agent and a reference set of images.
3. **EMVR for Bridge inspection EQA.** We propose a novel EQA method that formulates QA over a set of images as a traversal over an image-based scene graph (an MDP), enabling agents to dynamically select views, compare evidence, and answer. This approach yields improvements of 13.6% in condition rating accuracy, 29% in visual evidence grounding, and 12.5% in answer quality over non-navigational baselines.
4. **Baseline EQA evaluations.** We benchmark contemporary VLMs and EQA methods on BridgeEQA, establishing strong baselines and highlighting remaining challenges.

## 2. Related Work

### 2.1. Bridge Inspection

Bridge inspection is critical for structural safety and public welfare. According to the latest NBI data, nearly 40 % of

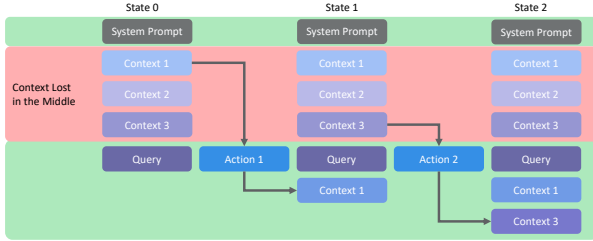


Figure 2. Illustration of how EMVR mitigates the “lost in the middle” problem. By navigating the scene graph and dynamically selecting relevant images, EMVR repositions critical visual evidence at the end of a VLM’s context window, reducing mid-sequence information loss.

U.S. bridges have reached or exceeded their 50-year design life, and over 10 % are subject to load restrictions because structural deterioration limits heavy vehicle access [5]. In the U.S., the National Bridge Inspection Standards (NBIS) mandate routine inspection of all public highway bridges longer than 20 ft at least every two years [15]. During each routine inspection, certified inspectors evaluate components such as the deck, superstructure, and substructure and assign condition ratings on a standardized 0–9 scale to help prioritize maintenance and rehabilitation [4, 15]. Achieving consistent ratings is challenging because inspectors must correctly interpret rating guidelines and synthesize the effects of local defects across the structure into a component-level assessment [15]. Although the guidelines are qualitative and rely heavily on inspector judgment, studies have found that expert inspectors typically agree within  $\pm 1$  condition rating [2]. The Bridge Inspector’s Reference Manual (BIRM) provides a step-by-step procedure for comparing field observations with rating criteria [39]. Recent advances in remote and autonomous inspection technologies [36, 38] and digital twin frameworks [18] now offer promising platforms for implementing AI-assisted assessment systems. However, none provide an end-to-end autonomous solution for bridge inspections using only images of the bridge mimicking an inspector.

## 2.2. Methods for Infrastructure Inspections

Existing approaches can be broadly grouped into three capabilities: *detection and classification*, *visual question answering*, and *report generation*. For detection, CLIP-based frameworks incorporating inspection knowledge, multi-view recognition models, and multi-class damage classifiers have been proposed to identify diverse defect types in bridge imagery [25, 41–43]. Other work leverages few-shot CLIP for semantically guided UAV inspections, transformer-based multi-modal fusion for surface and sub-surface damage segmentation, and instance segmentation of bridge point clouds [11, 31, 34]. For VQA, bridge-

specific vision-language pretraining using image-text pairs from inspection reports and multi-view VQA pipelines that integrate 3D reconstruction have been explored to support question answering and cause inference for observed damage [22, 45]. For report generation, image-to-text systems based on vision-language pretraining generate descriptive inspection narratives, while large-language-model-based frameworks produce structured maintenance plans from detected defects [32, 44]. Beyond bridges, VQA benchmarks targeting post-disaster and remote sensing scenarios provide additional testbeds for assessing vision-language capabilities in infrastructure and environmental contexts [29, 35, 40]. Despite these advances, most methods operate on single images or treat multiple images as independent inputs, and thus lack the ability to reason jointly over multiple views or synthesize spatial relationships between structural components.

## 2.3. Embodied Question Answering

Embodied Question Answering (EQA) answers natural language questions about environments by reasoning over spatially distributed observations [12, 30]. EQA encompasses two settings: episodic memory EQA (EM-EQA), where agents answer from pre-collected observations containing all required images, and *active EQA* (A-EQA), where agents explore autonomously [30]. The OpenEQA benchmark [30] established the first open-vocabulary EQA dataset with 180 real-world scenes and 1600 QAs. Existing benchmarks focus predominantly on household environments with simple spatial layouts and queries (object counting, color identification), lacking the multi-scale structure, heterogeneous conditions with real imaging, and domain-specific criteria of professional inspection tasks [8, 12, 13, 48].

Among EQA methods the Multi-Frame VLM [30] has consistently shown to be the strongest baseline across open-vocabulary EQA benchmarks with varying domains [24, 30, 48, 52]. As such we also use the Multi-Frame VLM method to establish a strong initial baseline. However, a weakness of this method is that all images are required as input to the VLM as context; as such, we theorize that this approach struggles with large image collections due to positional bias at long contexts where mid-sequence information is “lost in the middle” [6, 9, 19, 21, 23, 27]. For inspection scenarios with potentially 100’s of images in context, this bias would degrade answer quality and visual grounding drastically.

## 2.4. Scene Graphs for Spatial Reasoning

Scene graphs encode spatial and semantic relationships in environments, enabling symbolic reasoning for embodied agents. 3D scene graphs (3DSGs) [7] organize scenes hierarchically to support navigation and manipulation, with recent frameworks [1, 17, 37] using them to ground natural



Figure 3. Scene graph structure for bridge inspection. Nodes represent viewpoints with associated images, edges encode spatial and semantic relationships. VLM-generated labels shown in blue, edge relationships in gray.

language instructions in spatial reasoning. Complementary 3D vision-language models [20, 49, 51] improve semantic grounding, though typically on point-cloud representations. In infrastructure inspection, recent work has enabled natural-language queries over point-cloud scenes [10] and coordinated multi-agent drone inspection using 3D scene graphs [26]. However, unlike general domains where robust object detectors and semantic segmentation models enable object-centric scene graphs, bridge inspection lacks foundation models capable of densely detecting all structural components (e.g., bearings, expansion joints, specific deterioration patterns). This limitation necessitates using images as graph nodes rather than detected objects. Motivated by these works and constraints, we use image-based scene graphs as allocentric maps for dynamic context retrieval.

### 3. Methodology

#### 3.1. Scene Graph Formulation

We formalize bridge structures as navigable scene graphs constructed from inspection images. This structured representation enables the conversion of a set of images from an EM-EQA problem into an A-EQA problem allowing for systematic exploration by embodied agents.

A scene graph  $\mathcal{G} = (\mathcal{V}, \mathcal{E}, \mathcal{I})$  represents the physical bridge structure captured in inspection images, where:

- $\mathcal{V}$  is a set of nodes, each representing a distinct viewpoint with an associated image
- $\mathcal{E} \subseteq \mathcal{V} \times \mathcal{V}$  is a set of directed edges representing spatial or semantic relationships between viewpoints
- $\mathcal{I}$  is the set of all images of the bridge, with a bijective mapping between nodes and images ( $|\mathcal{V}| = |\mathcal{I}|$ )

Each node  $v \in \mathcal{V}$  encapsulates:

- **Image name:** The associated photograph capturing the bridge structure
- **Central focus:** A semantic label describing the primary bridge component or viewpoint, using inspector terminology (e.g., “Abutment 1 approach (South)”, “Span 1 deck and superstructure”)
- **Image description:** Detailed visual observations of structural elements and conditions

- **Edge set:** Connections to semantically or spatially related nodes

Edges  $(v_i, v_j) \in \mathcal{E}$  connect related viewpoints and include relationship descriptors (e.g., “opposite approach”, “supports span”, “contains bearings”). This graph structure, Figure 3, transforms unordered image collections into spatially-organized representations of the bridge structure that embodied agents can navigate.

**Scene Graph Construction.** Scene graphs are constructed automatically using Gemini 2.5 Flash and fall back to Gemini 2.5 Pro when parsing errors are detected. The scene graph output as a JSON structure with a `nodes` array, where each node contains:

- **image\_name:** Unique filename identifier for the image (e.g., `e23856c62fffb0.png`)
- **central\_focus:** Concise semantic label for the primary bridge component or viewpoint (e.g., “Superstructure steel girders and bearings at pier”)
- **image\_description:** Detailed visual observations of the bridge structure, including structural elements, defects, and contextual information (e.g., “View of the superstructure showing steel open girders and cross-frames supported by ...”)
- **edges:** Array of directed edge objects, each containing:
  - `connected_to`: Target image filename
  - `description_of_connection`: Natural language description of the semantic relationship

The natural language edge descriptions capture the following relationship patterns:

- **Hierarchical relationships:** Connecting overview and detail perspectives (e.g., “is a detailed view of”, “is an overview of a component detailed in”)
- **Structural relationships:** Physical support and load-bearing connections (e.g., “supports”, “is supported by”)
- **Spatial adjacency:** Neighboring components or locations (e.g., “is adjacent to”, “is an overview of the environment for”)
- **Condition similarity:** Viewpoints showing comparable defects or states (e.g., “shows similar condition to”)
- **Component membership:** Part-whole relationships within larger assemblies (e.g., “is a component of the deck shown in”)

#### 3.2. Embodied Memory Visual Reasoning

Embodied Memory Visual Reasoning frames the agent’s decision process as sequential navigation and selective recall, enabling it to retrieve and prioritize only the visual evidence needed to answer an inspection query. Figure 4 illustrates the complete EMVR framework: the scene graph  $\mathcal{G}$  provides the structural context for selective image access. Unlike EM-EQA baselines that receive all images simultaneously and respond in a single pass, EMVR initializes with only the scene graph structure (nodes, edges, semantic labels)

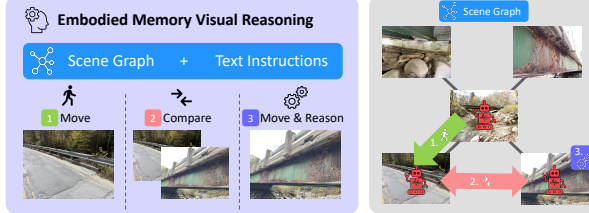


Figure 4. Overview of Embodied Memory Visual Reasoning. An agent operates in an environment with a scene graph serving as an allocentric map. The agent navigates via an MDP, retrieving images dynamically to bring only relevant information into context.

and then takes actions through an MDP to retrieve relevant visual context on demand.

We formulate the MDP as follows:

- **State Space:** At time step  $t$ , the agent’s state is  $s_t = (v_t, h_t)$  where  $v_t \in \mathcal{V}$  is the current node and  $h_t$  represents the interaction history including previously viewed images and observations.
- **Observation Space:** The agent has access to the complete scene graph structure  $\mathcal{G}$ , including all node central focus labels, image descriptions, and edge relationships. At each time step, the agent observes its current node  $v_t$  and can query neighboring nodes  $\mathcal{N}(v_t) = \{v_j \mid (v_t, v_j) \in \mathcal{E}\}$ .
- **Action Space:** The agent executes actions via function calls:
  - **MOVE( $v_j$ ):** Navigate to node  $v_j \in \mathcal{N}(v_t)$ , updating  $v_{t+1} = v_j$
  - **COMPARE( $\{v_i, v_j, \dots\}$ ):** Load and analyze images from two or more nodes for comparative inspection, where  $|\{v_i, v_j, \dots\}| \geq 2$
  - **REASON( $v_i$ ):** Perform self-questioning on a single image at node  $v_i$  to extract specific details
  - **RESPOND( $q$ ):** Generate an answer to the inspection query  $q$  with cited image references and a condition rating, ending the trajectory.
- **Policy:** A vision-language model implements policy  $\pi(a_t \mid s_t, q)$  that selects function calls based on the current state and inspection query. The policy terminates upon executing RESPOND.

### 3.3. Condition Rating Accuracy

The NBI condition rating scale [15] ranges from **0 (Failed)** to **9 (Excellent)**, with each integer representing a distinct condition category based on observable structural characteristics. We report *exact match* accuracy and *within  $\pm 1$*  accuracy. Exact matches between condition ratings for human inspectors are noisy, but there is a high agreement at  $\pm 1$  [2, 33] making it a more robust measure.

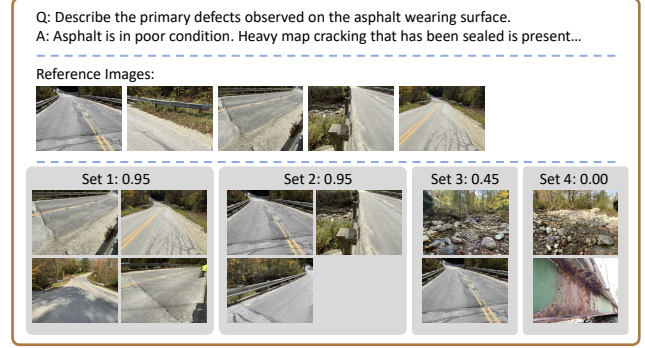


Figure 5. Example Image Citation Relevance scores for varying image citation sets. Multiple citation sets can provide equally valid supporting evidence.

### 3.4. Image Citation Relevance

Bridge inspectors justify condition ratings with photographic evidence. Similarly, Image Citation Relevance evaluates whether agents cite appropriate supporting images by semantically comparing agent selections against a reference set, Figure 5. To achieve this, we employ a VLM-as-a-judge approach with Gemini 2.5 Flash, chosen for its cost effectiveness and alignment with human preferences. The judge receives the question, the ground truth answer, reference images  $\mathcal{R}$  (as examples, not definitive ground truth), and agent-selected images  $\mathcal{R}_{\text{agent}}$ , then scores on a 0.0–1.0 scale while penalizing over-selection in the event that an agent cites more than 5 times the number of images in the reference set. On average, all EQA methods chose fewer than 6 images; as such, they were never penalized sharply. The final Image Citation Relevance score averages judge ratings across all evaluation questions. We validate this metric for human alignment using three annotators, showing a Spearman correlation of 0.817 between the averaged human annotations and the Image Citation Relevance score. Additional details on the evaluation of this metric against human alignment are provided in the appendix.

**Reference Image Citations** During dataset construction (Section 4.1), each question-answer pair is annotated with a set of reference images  $\mathcal{R} = \{i_1, i_2, \dots, i_k\}$  that provide visual evidence for the ground truth answer. These references are extracted from the original PDF inspection reports, where inspectors explicitly link textual condition descriptions to specific photographs. This annotation ensures that reference images represent inspector-validated visual evidence.

**Agent Image Citations** When answering an inspection query  $q$ , the agent generates a structured response that includes both a textual answer and an explicit list of supporting reference images  $\mathcal{R}_{\text{agent}} = \{i'_1, i'_2, \dots, i'_m\}$ . This struc-

tured output format requires agents to explicitly cite which images provide visual evidence for their condition assessment, mirroring the documentation requirements of professional inspection reports.

## 4. Dataset

The BridgeEQA dataset comprises 200 bridge inspection reports from the Vermont Agency of Transportation (VTrans), spanning 73 Vermont towns with 9,586 images (avg. 47.93 per report) and 2,200 question-answer pairs annotated with NBI condition ratings. We split our dataset into a train and test set of 1,100 QA pairs each.

### 4.1. Dataset Construction

We construct our dataset from unstructured PDF bridge inspection reports in the Vermont Agency of Transportation (VTrans) public database, where each report documents a single bridge with condition ratings, inspector notes, and photographs; the overall pipeline is summarized in Figure 6. After applying report-level, page-level, and image-level quality filters, including a minimum threshold of 20 images per report and the removal of low-information pages and thumbnails, we randomly sample 200 reports and extract both textual and visual content that meets these criteria, yielding 9,586 images and an average of 47.93 images per report.

In the transformation and validation stages, we use Gemini 2.5 Flash and Gemini 2.5 Pro as zero-shot parsers to structure text and images, map image references to inspector notes, and extract NBI condition ratings while preserving inspector rationale, with Gemini 2.5 Pro serving as a fallback when parsing errors or hallucinations are detected. We then validate the structured data with automated checks and human review, generate grounded QA pairs with image references and condition labels, and evaluate QA quality using RAGAs Faithfulness & Answer Relevancy [14], RAGalyst Answerability [16], and an LLM-as-a-Judge Inspector Relevancy score. We achieve a Faithfulness of 0.997, an Answer Relevancy of 0.997, an Answerability of 0.996, and an Inspector Relevancy of 0.980. Our human review of 100 QAs showed 100% accuracy. Additional implementation and validation details are provided in the appendix.

### 4.2. Geographic and Structural Coverage

The 200 inspection reports provide diverse coverage across bridge types (beam, truss, arch), construction materials (concrete, steel, timber, composite), environmental contexts (rural to urban, varying climatic exposure), and traffic conditions (low-volume rural routes to state highways), as shown in Figure 7. This diversity ensures models must generalize across varied contexts rather than overfit to specific bridge archetypes or environmental conditions.

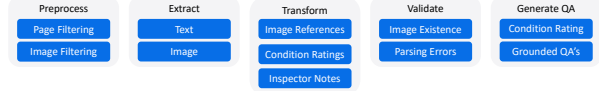


Figure 6. Pipeline for constructing the BridgeEQA dataset from Vermont Agency of Transportation (VTrans) inspection reports. Reports undergo preprocessing, extraction, transformation, validation, and QA generation stages to produce component-level question-answer pairs with NBI condition ratings and reference image citations.

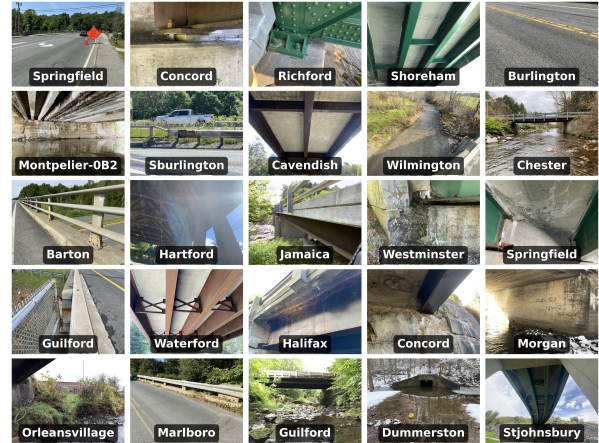


Figure 7. Representative sample images from BridgeEQA across Vermont bridges, demonstrating diverse bridge types (beam, truss, arch), construction materials, environmental conditions, and imaging perspectives.

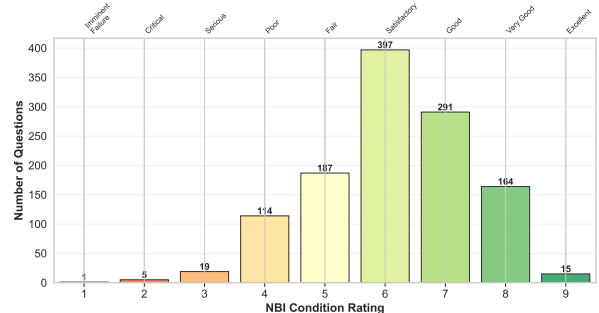


Figure 8. Distribution of NBI condition ratings for bridge components in the BridgeEQA dataset.

### 4.3. Condition Rating Distribution

The BridgeEQA dataset focuses on component-level condition assessments of bridge elements (decks, superstructures, substructures, abutments, wingwalls) using the NBI scale from 0 to 9, where higher ratings indicate better condition [15].

As shown in Figure 8, the distribution is centered around ratings 5-7 (Fair to Good), with rating 6 (Satisfactory) be-

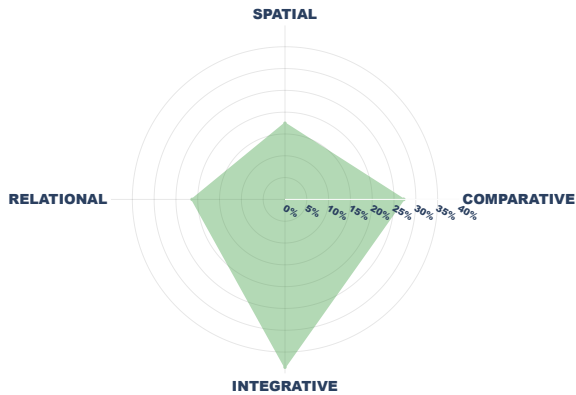


Figure 9. Distribution of question types in the BridgeEQA dataset (based on a random sample of 300 QA pairs). Each question can have multiple types simultaneously (e.g., both Comparative and Spatial), so percentages represent the proportion of questions containing each type and do not sum to 100%.

ing most common at 397 questions. This reflects the typical condition profile of aging infrastructure, where most components show minor deterioration but remain structurally sound. The dataset includes examples across the full rating spectrum (severely deteriorated components at ratings 1-4, excellent condition at ratings 8-9), enabling comprehensive evaluation of vision-language models’ ability to assess diverse infrastructure conditions.

#### 4.4. Question Type Categorization

To ensure question diversity we randomly sample 300 QA pairs and categorize the types of questions in BridgeEQA into one or more of the following types:

1. **Comparative:** Side-by-side comparison of structural elements (e.g., “Compare cracking severity on upstream versus downstream pier faces”).
2. **Spatial:** Location and distribution of deterioration patterns (e.g., “Where is spalling most concentrated on the deck surface?”).
3. **Relational:** Cause-effect reasoning about deterioration mechanisms (e.g., “What caused the corrosion on the beam ends near the joint?”).
4. **Integrative:** Cross-component synthesis across different element types (e.g., “How does deck condition compare to superstructure condition?”).

As shown in Figure 9, integrative reasoning (38.5%) and comparative analysis (27.2%) are most prevalent, with relational reasoning (21.3%) and spatial analysis (17.5%) also represented. Questions frequently combine multiple types.

Table 1. Answer Correctness across three VLMs and five methods.

Method	Gemini 2.5 Flash Lite	Gemini 2.5 Flash	Grok 4 Fast
Multi-Frame VLM [30]	0.507	0.484	0.576
Socratic LLM w/ SG [30, 47]	0.542	0.588	0.614
Multi-Frame VLM w/ SG [30]	<b>0.581</b>	0.548	0.622
EMVRVLM w/ SG Only	0.512	<b>0.609</b>	0.638
EMVRVLM w/ Images + SG	0.497	0.551	<b>0.648</b>

Table 2. Image Citation Relevance across three VLMs and five methods.

Method	Gemini 2.5 Flash Lite	Gemini 2.5 Flash	Grok 4 Fast
Multi-Frame VLM [30]	0.717	0.694	0.687
Socratic LLM w/ SG [30, 47]	0.775	0.767	0.838
Multi-Frame VLM w/ SG [30]	0.802	0.778	0.833
EMVRVLM w/ SG Only	0.798	<b>0.836</b>	0.876
EMVRVLM w/ Images + SG	<b>0.849</b>	0.803	<b>0.889</b>

## 5. Experiments

### 5.1. Experimental Setup

We evaluate five EQA methods following an experimental protocol aligned with prior open-vocabulary EQA work [24, 30, 48, 52]. As strong baselines, we include **Multi-Frame VLM** [30] and **Socratic LLM w/ SG** [30, 47], which have demonstrated consistently strong performance on existing open-vocabulary EQA benchmarks. We further augment Multi-Frame VLM with scene graph context, denoted **Multi-Frame VLM w/ SG** [30]. In addition, we compare against EMVRVLM with scene graphs only as initial context, **EMVRVLM w/ SG Only**, and with both images and scene graphs, **EMVRVLM w/ Images + SG**. To assess generalization across VLMs, we evaluate all methods with **Gemini 2.5 Flash Lite**, **Gemini 2.5 Flash**, and **Grok 4 Fast** on our test set of 1,100 QA pairs. To ensure fair comparisons, all methods were given the same prompt with context related to bridge inspections.

### 5.2. Quantitative Results

Figure 11 presents the condition rating prediction accuracy across all three VLMs and five methods. The results demonstrate that EMVRVLM improves performance across multiple metrics and models.

Tables 1 and 2 present comprehensive performance metrics across all configurations and models. The EMVRVLM w/ Images + SG configuration achieves strong performance across both metrics. For Answer Correctness, Grok 4 Fast reaches 0.648 while Gemini 2.5 Flash EMVRVLM w/ SG Only achieves 0.609. Particularly notable is the visual grounding performance: Grok 4 Fast EMVRVLM w/ Images + SG achieves 0.889 Image Citation Relevance, demonstrating strong capability in identifying relevant visual evidence.

**Bridge EQA Example**

**Question:** Describe the condition of the creosoted timber pier columns and provide their condition rating.. A numerical value for the condition rating is required. **Ground Truth Answer:** The pier columns consist of 4 heavy duty creosoted timber beams with minor vertical splitting, and cross bracing beam boards are in place. **This condition is considered SATISFACTORY with a rating of 6.**

Reference Image Citations



EMVR VLM with Images + SG (Grok 4 Fast)

Agent Image Citations



Answer Correctness: 0.8  
Image Citation Relevance: 0.95  
Generated Condition Rating: 7

**Agent Answer:** The creosoted timber pier columns on Pier 1 and Pier 2 show minor vertical splitting and surface checking from weathering and age. Creosote wear exposes some wood to minor degradation, but no rot, extensive cracking, deformation, or structural compromise is evident, with intact cross-bracing on stable concrete foundations. Overall, the columns are in good condition with only limited minor issues.

**Multi-Frame VLM (Grok 4 Fast)**

Agent Image Citations



Answer Correctness: 0.0  
Image Citation Relevance: 0.0  
Generated Condition Rating: 3

**Agent Answer:** The creosoted timber pier columns in the substructure bents exhibit advanced deterioration, including extensive splitting, checking, surface erosion, dark creosote staining, localized rot pockets, and soft spots from moisture ingress and possible fungal or insect damage. Cross-bracing remains intact but weathered. The overall substructure condition is serious, compromising structural capacity and requiring priority repairs or replacement.

EMVR VLM (Gemini 2.5 Flash)

Agent Image Citations



Answer Correctness: 0.0  
Image Citation Relevance: 0.0  
Generated Condition Rating: 3

**Agent Answer:** The concrete piling exhibit large spalls with exposed reinforcing steel and heavy corrosion, along with horizontal and vertical cracking clearly visible. This deterioration significantly affects the structural integrity.

Hallucinated Image Citations



Figure 10. We observed several qualitative performance patterns. We provide a correct example and contrast this with two commonly observed failure cases - poor image citation and hallucinate image citations. These failure cases indicate that low quality image citations can be a proxy for detecting the occurrence of hallucinations or poor answer generations.

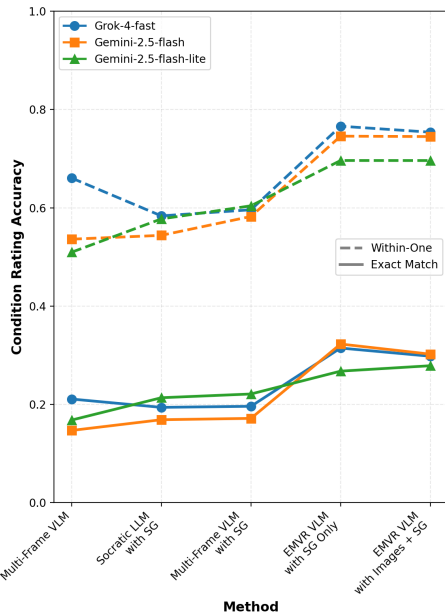


Figure 11. Condition rating prediction accuracy comparison across varying models and methods. Expert inspectors demonstrate 98% consistency between assigned ratings when ratings fall within  $\pm 1$  of a median rating [2, 3].

### 5.3. Error Analysis and Failure Modes

We perform a qualitative analysis, presented in Figure 10, where we showcase a successful example and contrast it with two commonly observed failure cases. In the successful example, the agent identifies the correct substructure and uses relevant image citations to ground its answer, achieving a condition rating within  $\pm 1$  of the ground truth. Conversely, we identified two primary failure modes that account for the large majority of incorrect condition assess-

ments. The first is poor image citations, where the agent cites irrelevant images, leading to an incorrect answer and rating. The second is hallucinated image citations, where a VLM invents citations for images that do not exist, resulting in nonsensical generations. These findings indicate that low quality image citations can be a proxy for detecting the occurrence of hallucinations or poor answer generations.

### 5.4. Limitations

While we tested several sub-30B-parameter VLMs, they could not reliably adhere to the required structured-output and function-calling protocol, so we excluded them from the main comparison to avoid unfair evaluations. The dataset size also limits the range of experiments we can run: each question is paired with an average of 47.93 images, so exhaustively exploring all model choices, context configurations, and EMVR variants would be computationally prohibitive, with our final experiments already processing an estimated 2.2 billion tokens. As a result, we focus on a representative subset of configurations and leave systematic evaluations of finetuning, action space design, additional EQA methods, and further context variations to future work.

## 6. Conclusion

In this work, we introduced **BridgeEQA**, a real-world Embodied Question Answering benchmark grounded in professional bridge inspection, comprising 2,200 question-answer pairs across 200 bridge scenes with 9,586 images. By leveraging egocentric imagery, expert-authored reports, and standardized NBI condition ratings, the dataset provides a testbed for evaluating spatial reasoning and multi-scale evidence aggregation in a domain with measurable expert-level criteria. To assess visual grounding, we proposed **Image Citation Relevance**, a metric that measures semantic alignment between agent-cited images and reference evi-

dence sets. We further presented Embodied Memory Visual Reasoning (**EMVR**), an EQA method that reformulates Episodic Memory EQA as traversal over an image-based scene graph, enabling dynamic context retrieval rather than fixed long-context input. Evaluations show improvements with EMVR across metrics. Using Grok 4 Fast, we find that EMVR improves condition rating accuracy within  $\pm 1$  by 9.3 percentage point, Image Citation Relevance by 20.2 percentage point, and Answer Correctness by 7.2 percentage point over the Multi-Frame VLM baseline. We hope our work jointly advances open-vocabulary EQA toward practical deployment in domains such as bridge inspection and supports future research on EQA-driven automated inspection for a safer tomorrow.

## 7. Acknowledgments

The authors would like to acknowledge partial financial support from the Texas Department of Transportation grant number 0-7181. The contents of this paper reflect the views of the authors, who are responsible for the facts and the accuracy of the data presented herein. The contents do not necessarily reflect the official views or policies of the sponsors.

## References

- [1] C. Agia et al. Taskography: Evaluating robot task planning over large 3d scene graphs. In *Conference on Robot Learning*, pages 46–58. PMLR, 2022. 3
- [2] Anil K Agrawal, Glenn A Washer, Xu Gong, et al. Consistency of the new york state bridge inspection program. Technical report, New York (NY). Dept. of Transportation, 2013. 3, 5, 8
- [3] Anil Kumar Agrawal, Glenn Washer, Sreenivas Alampalli, Xu Gong, and Ran Cao. Evaluation of the consistency of bridge inspection ratings in new york state. *Journal of Infrastructure Systems*, 27(3):04021016, 2021. 8
- [4] A. S. Ahmad. Bridge preservation guide: Maintaining a state of good repair using cost-effective investment strategies. Technical report, United States. Federal Highway Administration, 2011. 3
- [5] American Society of Civil Engineers. *2021 Report Card for America’s Infrastructure*. ASCE, Reston, VA, 2021. 2, 3
- [6] Shengnan An, Zexiong Ma, Zeqi Lin, Nanning Zheng, and Jian-Guang Lou. Make your llm fully utilize the context. *ArXiv*, abs/2404.16811, 2024. 2, 3
- [7] I. Armeni et al. 3d scene graph: A structure for unified semantics, 3d space, and camera. In *Proceedings of the IEEE/CVF International Conference on Computer Vision (ICCV)*, pages 5664–5673, 2019. 3
- [8] Daichi Azuma, Taiki Miyanishi, Shuhei Kurita, and Motoaki Kawanabe. Scanqa: 3d question answering for spatial scene understanding. In *proceedings of the IEEE/CVF conference on computer vision and pattern recognition*, pages 19129–19139, 2022. 3
- [9] Yushi Bai, Xin Lv, Jiajie Zhang, Hong Lyu, Jiankai Tang, Zhidian Huang, Zhengxiao Du, Xiao Liu, Aohan Zeng, Lei Hou, Yuxiao Dong, Jie Tang, and Juanzi Li. Longbench: A bilingual, multitask benchmark for long context understanding. *ArXiv*, abs/2308.14508, 2023. 2, 3
- [10] Y. Chen, S. Zhang, T. Han, Y. Du, W. Zhang, and J. Li. Chat3d: Interactive understanding of 3d scene-level point clouds by chatting with foundation models for urban ecological construction. *ISPRS Journal of Photogrammetry and Remote Sensing*, 212:181–192, 2024. 4
- [11] Z. Chen, Y. Zou, V. A. Gonzalez, J. Ingham, and L. M. Wotherspoon. Bridge inspection using a multi-modal vision language model. In *Proceedings of the 6th International Conference on Civil and Building Engineering Informatics*, page 11, 2025. 3
- [12] Abhishek Das, Samyak Datta, Georgia Gkioxari, Stefan Lee, Devi Parikh, and Dhruv Batra. Embodied question answering. In *Proceedings of the IEEE conference on computer vision and pattern recognition*, pages 1–10, 2018. 2, 3
- [13] Vishnu Sashank Dorbala, Prasoon Goyal, Robinson Piramuthu, Michael Johnston, Reza Ghanadhan, and Dinesh Manocha. Is the house ready for sleeptime? generating and evaluating situational queries for embodied question answering. *arXiv preprint arXiv:2405.04732*, 2024. 3
- [14] Shahul Es, Jithin James, Luis Espinosa Anke, and Steven Schockaert. RAGAs: Automated evaluation of retrieval augmented generation. In *Proceedings of the 18th Conference of the European Chapter of the Association for Computational Linguistics: System Demonstrations*, pages 150–158, St. Julians, Malta, 2024. Association for Computational Linguistics. 6
- [15] Federal Highway Administration. Recording and coding guide for the structure inventory and appraisal of the nation’s bridges. Technical Report FHWA-PD-96-001, U.S. Department of Transportation, Federal Highway Administration, 1995. 2, 3, 5, 6
- [16] Joshua Gao, Quoc Huy Pham, Subin Varghese, Silwal Saurav, and Vedhus Hoskere. Ragalyst: Automated human-aligned agentic evaluation for domain-specific rag. *arXiv preprint arXiv:2511.04502*, 2025. 6
- [17] Q. Gu et al. Conceptgraphs: Open-vocabulary 3d scene graphs for perception and planning. In *IEEE International Conference on Robotics and Automation (ICRA)*, pages 5021–5028, 2024. 3
- [18] Vedhus Hoskere, Delaram Hassanlou, Asad Ur Rahman, Reza Bazrgary, and Muhammad Taseer Ali. Unified framework for digital twins of bridges. *Automation in Construction*, 175:106214, 2025. 3
- [19] Cheng-Ping Hsieh, Simeng Sun, Samuel Kriman, Shantanu Acharya, Dima Rekesh, Fei Jia, and Boris Ginsburg. Ruler: What’s the real context size of your long-context language models? *ArXiv*, abs/2404.06654, 2024. 2, 3
- [20] B. Jia et al. Sceneneverse: Scaling 3d vision-language learning for grounded scene understanding. In *Computer Vision - ECCV 2024*, pages 289–310. Springer Nature Switzerland, 2025. 4
- [21] Huiqiang Jiang, Qianhui Wu, Xufang Luo, Dongsheng Li, Chin-Yew Lin, Yuqing Yang, and Lili Qiu. Longllmelingua:

Accelerating and enhancing llms in long context scenarios via prompt compression. In *Annual Meeting of the Association for Computational Linguistics*, 2023. 2, 3

[22] T. Kunlamai, T. Yamane, M. Suganuma, P. Chun, and T. Okatani. Improving visual question answering for bridge inspection by pre-training with external image-text data. *Computer-Aided Civil and Infrastructure Engineering*, 39(3):345–361, 2024. 3

[23] Yuri Kuratov, A. Bulatov, Petr Anokhin, Ivan Rodkin, Dmitry Sorokin, Artyom Y. Sorokin, and M. Burtsev. Babilong: Testing the limits of llms with long context reasoning-in-a-haystack. *ArXiv*, abs/2406.10149, 2024. 2, 3

[24] Yifan Li, Yuhang Chen, Anh Dao, Lichi Li, Zhongyi Cai, Zhen Tan, Tianlong Chen, and Yu Kong. Industreqa: Pushing the frontiers of embodied question answering in industrial scenarios. *arXiv preprint arXiv:2505.20640*, 2025. 3, 7

[25] P. Liao and G. Nakano. Bridgeclip: Automatic bridge inspection by utilizing vision-language model. In *International Conference on Pattern Recognition*, pages 61–76. Springer, 2024. 3

[26] J. Liu, H. Li, C. Chai, K. Chen, and D. Wang. A llm-informed multi-agent ai system for drone-based visual inspection for infrastructure. *Advanced Engineering Informatics*, 68:103643, 2025. 4

[27] Nelson F. Liu, Kevin Lin, John Hewitt, Ashwin Paranjape, Michele Bevilacqua, F. Petroni, and Percy Liang. Lost in the middle: How language models use long contexts. *Transactions of the Association for Computational Linguistics*, 12:157–173, 2023. 2, 3

[28] Yuan Liu, Haodong Duan, Yuanhan Zhang, Bo Li, Songyang Zhang, Wangbo Zhao, Yike Yuan, Jiaqi Wang, Conghui He, Ziwei Liu, et al. Mmbench: Is your multi-modal model an all-around player? In *European conference on computer vision*, pages 216–233. Springer, 2024. 2

[29] S. Lobry, D. Marcos, J. Murray, and D. Tuia. Rsvqa: Visual question answering for remote sensing data. *IEEE Transactions on Geoscience and Remote Sensing*, 58(12):8555–8566, 2020. 3

[30] Arjun Majumdar, Anurag Ajay, Xiaohan Zhang, Pranav Putta, Sriram Yenamandra, Mikael Henaff, Sneha Silwal, Paul Mcvay, Oleksandr Maksymets, Sergio Arnaud, Karmesh Yadav, Qiyang Li, Ben Newman, Mohit Sharma, Vincent Berge, Shiqi Zhang, Pulkit Agrawal, Yonatan Bisk, Dhruv Batra, Mrinal Kalakrishnan, Franziska Meier, Chris Paxton, Alexander Sax, and Aravind Rajeswaran. Openeqa: Embodied question answering in the era of foundation models. In *2024 IEEE/CVF Conference on Computer Vision and Pattern Recognition (CVPR)*, pages 16488–16498, 2024. 2, 3, 7

[31] Lokeswari Malepati, Vedhus Hoskere, Nagarajan Ganapathy, and S Suriya Prakash. Segmentation of surface and subsurface damages in concrete structures through fusion of multi-modal images using vision transformer. *Automation in Construction*, 179:106469, 2025. 3

[32] I. S. Mohamed and A. Y. A. Omaisan. Infragpt smart infrastructure: An end-to-end vlm-based framework for detecting and managing urban defects. *arXiv preprint arXiv:2510.16017*, 2025. 3

[33] Mark Moore, Brent M Phares, Benjamin Graybeal, Dennis Rolander, Glenn Washer, Janney Wiss, et al. Reliability of visual inspection for highway bridges, volume i. Technical report, Turner-Fairbank Highway Research Center, 2001. 5

[34] Asad Ur Rahman and Vedhus Hoskere. Instance segmentation of reinforced concrete bridge point clouds with transformers trained exclusively on synthetic data. *Automation in Construction*, 173:106067, 2025. 3

[35] M. Rahnemoonfar, T. Chowdhury, A. Sarkar, D. Varshney, M. Yari, and R. R. Murphy. Floodnet: A high resolution aerial imagery dataset for post-flood scene understanding. *IEEE Access*, 9:89644–89654, 2021. 3

[36] Anna M Rakoczy, Diogo Ribeiro, Vedhus Hoskere, Yasutaka Narazaki, Piotr Olaszek, Wojciech Karwowski, Rafael Cabral, Yanlin Guo, Marcos Massao Futai, Pietro Milillo, et al. Technologies and platforms for remote and autonomous bridge inspection—review. *Structural Engineering International*, 35(3):354–376, 2025. 3

[37] K. Rana, J. Haviland, S. Garg, J. Abou-Chakra, I. Reid, and N. Suenderhauf. Sayplan: Grounding large language models using 3d scene graphs for scalable robot task planning. *arXiv preprint arXiv:2307.06135*, 2023. 3

[38] Diogo Ribeiro, Anna M Rakoczy, Rafael Cabral, Vedhus Hoskere, Yasutaka Narazaki, Ricardo Santos, Gledson Tondo, Luis Gonzalez, José Campos Matos, Marcos Massao Futai, et al. Methodologies for remote bridge inspection. *Sensors (Basel, Switzerland)*, 25(18):5708, 2025. 3

[39] T. W. Ryan, R. A. Hrtle, J. E. Mann, and L. J. Danovich. Bridge inspector’s reference manual. Technical report, National Highway Institute (US), 2006. 2, 3

[40] A. Sarkar, T. Chowdhury, R. R. Murphy, A. Gangopadhyay, and M. Rahnemoonfar. Sam-vqa: Supervised attention-based visual question answering model for post-disaster damage assessment on remote sensing imagery. *IEEE Transactions on Geoscience and Remote Sensing*, 61:1–16, 2023. 3

[41] Deepank Kumar Singh, Vedhus Hoskere, and Pietro Milillo. Multiclass post-earthquake building assessment integrating high-resolution optical and sar satellite imagery, ground motion, and soil data with transformers. *Earthquake Spectra*, page 87552930251377778, 2025. 3

[42] Subin Varghese and Vedhus Hoskere. View-invariant pixel-wise anomaly detection in multi-object scenes with adaptive view synthesis. *arXiv preprint arXiv:2406.18012*, 2024.

[43] Subin Varghese, Joshua Gao, and Vedhus Hoskere. Viewdelta: Scaling scene change detection through text-conditioning. In *Proceedings of the IEEE/CVF International Conference on Computer Vision (ICCV) Workshops*, 2025, 2025. 3

[44] S. Wang and N. El-Gohary. Automated bridge inspection image interpretation based on vision-language pre-training. In *Computing in Civil Engineering 2023*, pages 1–8, 2024. 3

[45] T. Yamane, P. Chun, J. Dang, and T. Okatani. Deep learning-based bridge damage cause estimation from multiple images using visual question answering. *Structure and Infrastructure Engineering*, pages 1–14, 2024. 3

- [46] Jihan Yang, Shusheng Yang, Anjali W. Gupta, Rilyn Han, Fei-Fei Li, and Saining Xie. Thinking in space: How multimodal large language models see, remember, and recall spaces. *2025 IEEE/CVF Conference on Computer Vision and Pattern Recognition (CVPR)*, pages 10632–10643, 2024. [2](#)
- [47] Andy Zeng, Maria Attarian, Brian Ichter, Krzysztof Choromanski, Adrian Wong, Stefan Welker, Federico Tombari, Aveek Purohit, Michael Ryoo, Vikas Sindhwani, et al. Socratic models: Composing zero-shot multimodal reasoning with language. *arXiv preprint arXiv:2204.00598*, 2022. [7](#)
- [48] Yong Zhao, Kai Xu, Zhengqiu Zhu, Yue Hu, Zhiheng Zheng, Yingfeng Chen, Yatai Ji, Chen Gao, Yong Li, and Jincai Huang. Cityeqa: A hierarchical llm agent on embodied question answering benchmark in city space. *arXiv preprint arXiv:2502.12532*, 2025. [3](#), [7](#)
- [49] H. Zhen et al. 3d-vla: A 3d vision-language-action generative world model. *arXiv preprint arXiv:2403.09631*, 2024. [4](#)
- [50] Lianmin Zheng, Wei-Lin Chiang, Ying Sheng, Siyuan Zhuang, Zhanghao Wu, Yonghao Zhuang, Zi Lin, Zhuohan Li, Dacheng Li, Eric Xing, et al. Judging llm-as-a-judge with mt-bench and chatbot arena. *Advances in neural information processing systems*, 36:46595–46623, 2023. [2](#)
- [51] Z. Zhu, X. Ma, Y. Chen, Z. Deng, S. Huang, and Q. Li. 3d-vista: Pre-trained transformer for 3d vision and text alignment. In *Proceedings of the IEEE/CVF International Conference on Computer Vision (ICCV)*, pages 2899–2909, 2023. [4](#)
- [52] Filippo Ziliotto, Tommaso Campari, Luciano Serafini, and Lamberto Ballan. Tango: Training-free embodied ai agents for open-world tasks. *2025 IEEE/CVF Conference on Computer Vision and Pattern Recognition (CVPR)*, pages 24603–24613, 2024. [3](#), [7](#)